

Encapsulation of Phthalocyanines in Biodegradable Poly(sebacic anhydride) Nanoparticles

Jie Fu,^{†,‡} Xi-you Li,[†] Dennis K. P. Ng,^{*,†} and Chi Wu^{*,†,§}

Department of Chemistry, The Chinese University of Hong Kong, Shatin, N. T., Hong Kong, China, College of Material Science and Engineering, Wuhan University of Technology, Wuhan, Hubei, China, and The Open Laboratory of Bond-selective Chemistry, Department of Chemical Physics, University of Science and Technology of China, Hefei, Anhui, China

Received December 6, 2001. In Final Form: February 20, 2002

A new series of phthalocyanine-containing biodegradable copolymers, namely poly(phthalocyanine-co-sebacic anhydride) (Pc-SA), have been synthesized. For copolymers with a low Pc content, the Pc rings exist mainly as monomeric species in chloroform, while the aggregation of these macrocycles becomes significant as the Pc content increases. Nanoparticles with an average hydrodynamic radius of 166 nm have been prepared from the copolymer Pc-SA-5, which has a Pc to sebacic acid molar ratio of 0.01, via a microphase inversion method. The collapse of polymer chains in the formation of Pc-SA-5 nanoparticles leads to aggregation of the Pc rings inside. The aggregation tendency decreases upon degradation of the nanoparticles in alkaline media, giving ultimately monomeric species. The degradation kinetics of Pc-SA-5 nanoparticles have been investigated by a combination of static and dynamic laser light scattering. It has been found that the rate of degradation increases with the pH and temperature. By using absorption and fluorescence spectroscopies, the release of Pc can be monitored, which occurs almost simultaneously with the degradation. The results suggest that this novel polymer-based colloidal system is potentially useful for the delivery and release of photosensitizers in photodynamic therapy.

Introduction

Photodynamic therapy (PDT), which was first developed for cancer treatment, is being actively exploited in many other clinical applications such as the treatment of age-related macular degeneration, hardening of arteries, sun-induced precancerous skin lesions, and wound infections.¹ The treatment involves administration of a photosensitive drug which has a high affinity to malignant tissues. It unleashes singlet oxygen as the predominant cytotoxic agent when excited by light of appropriate wavelength and power. Among the various photosensitizers being investigated,² phthalocyanines have found to be highly promising.^{2,3} Owing to their strong Q band absorptions at the red visible region (ca. 700 nm with $\epsilon \approx 10^5 \text{ mol}^{-1} \text{ dm}^3 \text{ cm}^{-1}$), these pigments can be excited at longer wavelengths than porphyrin-based photosensitizers such as Photofrin, which is the first clinically approved photosensitizer. This optical property allows a deeper penetration of light into tissues.⁴ The macrocycles are also relatively nontoxic in

the dark and have relatively high singlet oxygen quantum yields.⁵ These unique features, together with their ease of functionalization and formulation, have aroused intense interest in the use of these functional dyes as second-generation photosensitizers in PDT.

One of the problems in using phthalocyanines in PDT arises from their intrinsic tendency toward aggregation.⁶ This intermolecular association process promotes the nonradiative internal conversion, almost invariably causing a shortening of the triplet lifetime and a drastic reduction of the overall photosensitizing efficiency.^{4,7} This problem is particularly serious in polar media such as water, which tends to self-associate and repels the hydrophobic π systems to form aggregates.⁸ Hydrophilic and nonaggregated phthalocyanines are therefore of special importance and have received much current attention.⁹ One of the strategies to reduce the aggregation of phthalocyanines in aqueous media involves the use of surfactants or other substances which can create a microheterogeneous environment such as micelle or liposome.^{9b-d} It has been found that phthalocyanines exist mainly as monomeric species in these environments, giving a

* To whom correspondence should be addressed. Fax: (852) 2603 5057. E-mail: dkpn@cuhk.edu.hk (D.K.P.N.); chiwu@cuhk.edu.hk (C.W.).

[†] The Chinese University of Hong Kong.

[‡] Wuhan University of Technology.

[§] University of Science and Technology of China.

(1) (a) Milgrom, L.; MacRobert, S. *Chem. Br.* **1998**, May, 45. (b) Rouhi, A. M. *Chem. Eng. News* **1998**, Nov 2, 22. (c) Dougherty, T. J.; Gomer, C. J.; Henderson, B. W.; Jori, G.; Kessel, D.; Korbelik, M.; Moan, J.; Peng, Q. *J. Natl. Cancer Inst.* **1998**, *90*, 889. (d) Sharman, W. M.; Allen, C. M.; van Lier, J. E. *Drug Discovery Today* **1999**, *4*, 507. (e) Bonnett, R. *Chemical Aspects of Photodynamic Therapy*; Gordon and Breach: Amsterdam, 2000. (f) MacDonald, I. J.; Dougherty, T. J. *J. Porphyrins Phthalocyanines* **2001**, *5*, 105.

(2) Ali, H.; van Lier, J. E. *Chem. Rev.* **1999**, *99*, 2379.

(3) (a) Rosenthal, I.; Ben-Hur, E. In *Phthalocyanines—Properties and Applications*; Leznoff, C. C., Lever, A. B. P., Eds.; VCH: New York, 1989; Vol. 1, pp 393–425. (b) Rosenthal, I. In *Phthalocyanines—Properties and Applications*; Leznoff, C. C., Lever, A. B. P., Eds.; VCH: New York, 1996; Vol. 4, pp 481–514. (c) Lukyanets, E. A. *J. Porphyrins Phthalocyanines* **1999**, *3*, 424. (d) Allen, C. M.; Sharman, W. M.; van Lier, J. E. *J. Porphyrins Phthalocyanines* **2001**, *5*, 161.

(4) Jori, G. *J. Photochem. Photobiol. A: Chem.* **1992**, *62*, 371.

(5) (a) Spikes, J. D.; van Lier, J. E.; Bommer, J. C. *J. Photochem. Photobiol. A: Chem.* **1995**, *91*, 193. (b) Foley, S.; Jones, G.; Liuzzi, R.; McGarvey, D. J.; Perry, M. H.; Truscott, T. G. *J. Chem. Soc., Perkin Trans. 2* **1997**, 1725. (c) Spiller, W.; Kliesch, H.; Wöhrle, D.; Hackbarth, S.; Röder, B.; Schnurpfeil, G. *J. Porphyrins Phthalocyanines* **1998**, *2*, 145.

(6) Choi, M. T. M.; Li, P. P. S.; Ng, D. K. P. *Tetrahedron* **2000**, *56*, 3881 and references therein.

(7) (a) Dhami, S.; Phillips, D. *J. Photochem. Photobiol. A: Chem.* **1996**, *100*, 77. (b) Howe, L.; Zhang, J. Z. *J. Phys. Chem. A* **1997**, *101*, 3207. (c) Lang, K.; Kubát, P.; Mosinger, J.; Wagnerová, D. M. *J. Photochem. Photobiol. A: Chem.* **1998**, *119*, 47. (d) Ball, D. J.; Wood, S. R.; Vernon, D. I.; Griffiths, J.; Dubbelman, T. M. A. R.; Brown, S. B. *J. Photochem. Photobiol. B: Biol.* **1998**, *45*, 28. (e) Howe, L.; Zhang, J. Z. *Photochem. Photobiol.* **1998**, *67*, 90.

(8) (a) Schelly, Z. A.; Harward, D. J.; Hemmes, P.; Eyring, E. M. *J. Phys. Chem.* **1970**, *74*, 3040. (b) Yang, Y.-C.; Ward, J. R.; Seiders, R. P. *Inorg. Chem.* **1985**, *24*, 1765.

relatively high photoactivity. These systems, however, suffer from low stability, low localizing property, and biocompatibility, which limit their use as photosensitizer carriers in PDT. The development of advanced delivery systems which can target malignant tissues and can preserve the photosensitizing ability of phthalocyanines thus remains as a challenging task.

Recently, polymer-based colloidal drug delivery and release systems, in particular those with biocompatible and biodegradable polymer backbones, have been studied extensively.¹⁰ By the incorporation of site-specific moieties or simply regulating the particle size, these systems are able to target different organs and control the release of drugs.^{10e,11} The surface of particles, for example, can be modified with poly(ethylene oxide) to improve the carriers' biocompatibility and biodistribution.^{10e,12} Although the use of polymeric particles for the delivery of various chemotherapeutic drugs is well-documented,¹³ entrapping phthalocyanines in these systems for targeted PDT has been little studied.¹⁴ In this paper, we describe a novel series of copolymers of a Zn(II) phthalocyanine and sebacic anhydride, which is a common building block of biocompatible and biodegradable polymers,^{10f,15} and the nanoparticle formation of one of these copolymers. The preparation, spectroscopic properties, and degradation kinetics of these systems, as studied by static and dynamic laser light scattering, are reported herein.

Experimental Section

General. Tetrahydrofuran (THF) and diethyl ether were distilled from sodium benzophenone ketyl. Toluene and *n*-hexane

(9) (a) Ng, A. C. H.; Li, X.-y.; Ng, D. K. P. *Macromolecules* **1999**, *32*, 5292 and references therein. (b) Li, X.-y.; He, X.; Ng, A. C. H.; Wu, C.; Ng, D. K. P. *Macromolecules* **2000**, *33*, 2119 and references therein. (c) Ngai, T.; Zhang, G.-Z.; Li, X.-y.; Ng, D. K. P.; Wu, C. *Langmuir* **2001**, *17*, 1381. (d) Chen, Z.; Li, X.-y.; Ngai, T.; Wu, C.; Ng, D. K. P. *Langmuir* **2001**, *17*, 7957.

(10) (a) *Polymeric Drugs and Drug Administration*; Ottenbrite, R. M., Ed.; American Chemical Society: Washington, DC, 1994. (b) *Controlled Drug Delivery: Challenges and Strategies*; Park, K., Ed.; American Chemical Society: Washington, DC, 1997. (c) Anderson, J. M.; Shive, M. S. *Adv. Drug Delivery Rev.* **1997**, *28*, 5. (d) Gan, Z.; Jim, T. F.; Li, M.; Yuer, Z.; Wang, S.; Wu, C. *Macromolecules* **1999**, *32*, 590. (e) Yang, L.; Alewandridis, P. *Curr. Opin. Colloid Interface Sci.* **2000**, *5*, 132. (f) Langer, R. *Acc. Chem. Res.* **2000**, *33*, 94.

(11) (a) Scholes, P. D.; Coombes, A. G. A.; Davies, M. C.; Illum, L.; Davis, S. S. In *Controlled Drug Delivery: Challenges and Strategies*; Park, K., Ed.; American Chemical Society: Washington, DC, 1997; pp 73–106. (b) Kong, G.; Braun, R. D.; Dewhirst, M. W. *Cancer Res.* **2000**, *60*, 4440.

(12) *Poly(ethylene glycol) Chemistry and Biological Applications*; Harris, J. M., Zalipsky, S., Eds.; American Chemical Society: Washington, DC, 1997.

(13) See, for example: (a) Kim, J. H.; Emoto, K.; Iijima, M.; Nagasaki, Y.; Aoyagi, T.; Okano, T.; Sakurai, Y.; Kataoka, K. *Polym. Adv. Technol.* **1999**, *10*, 647. (b) Nishiyama, N.; Yokoyama, M.; Aoyagi, T.; Okano, T.; Sakurai, Y.; Kataoka, K. *Langmuir* **1999**, *15*, 377. (c) Yokoyama, M.; Okano, T.; Sakurai, Y.; Fukushima, S.; Okamoto, K.; Kataoka, K. *J. Drug Targeting* **1999**, *7*, 171. (d) Kataoka, K.; Matsumoto, T.; Yokoyama, M.; Okano, T.; Sakurai, Y.; Fukushima, S.; Okamoto, K.; Kwon, G. S. *J. Controlled Release* **2000**, *64*, 143. (e) Jung, T.; Kamm, W.; Breitenbach, A.; Kaiserling, E.; Xiao, J. X.; Kissel, T. *Eur. J. Pharm. Biopharm.* **2000**, *50*, 147. (f) Wang, D.; Kopecková, P.; Minko, T.; Nanayakkara, V.; Kopecek, J. *Biomacromolecules* **2000**, *1*, 313.

(14) (a) Labib, A.; Lenaerts, V.; Chouinard, F.; Leroux, J. C.; Ouellet, R.; van Lier, J. E. *Pharm. Res.* **1991**, *8*, 1027. (b) Allemann, E.; Rousseau, J.; Brasseur, N.; Kudrevich, S. V.; Lewis, K.; van Lier, J. E. *Int. J. Cancer* **1996**, *66*, 821. (c) Leroux, J. C.; Allemann, E.; DeJaeghere, F.; Doelker, E.; Gurny, R. *J. Controlled Release* **1996**, *39*, 339. (d) Taillefer, J.; Jones, M.-C.; Brasseur, N.; van Lier, J. E.; Leroux, J.-C. *J. Pharm. Sci.* **2000**, *89*, 52. (e) Taillefer, J.; Brasseur, N.; van Lier, J. E.; Lenaerts, V.; Le Garrec, D.; Leroux, J.-C. *J. Pharm. Pharmacol.* **2001**, *53*, 155.

(15) See, for example: (a) Teomim, D.; Fishbien, I.; Golomb, G.; Orloff, L.; Mayberg, M.; Domb, A. J. *J. Controlled Release* **1999**, *60*, 129. (b) Jiang, H. L.; Zhu, K. J. *Int. J. Pharm.* **2000**, *194*, 51. (c) Wu, C.; Fu, J.; Zhao, Y. *Macromolecules* **2000**, *33*, 9040. (d) Fu, J.; Wu, C. *J. Polym. Sci. B, Polym. Phys.* **2001**, *39*, 703. (e) Qiu, L. Y.; Zhu, K. J. *Int. J. Pharm.* **2001**, *219*, 151. (f) Teomim, D.; Domb, A. J. *Biomacromolecules* **2001**, *2*, 37. (g) Shen, E.; Piszczek, R.; Dziadul, B.; Narasimhan, B. *Biomaterials* **2001**, *22*, 201.

Table 1. Weight-Average Molecular Weight (M_w) and Fluorescence Quantum Yield (Φ_f) of Phthalocyanine-containing Polymers Pc-SA-*n* (*n* = 1–5)

polymer	molar ratio of 1:sebacic acid	M_w^a (g mol ⁻¹)	Φ_f^b
Pc-SA-1	5.60×10^{-4}	4.59×10^4	0.32
Pc-SA-2	1.11×10^{-3}	1.22×10^5	0.26
Pc-SA-3	2.15×10^{-3}	3.35×10^5	0.22
Pc-SA-4	4.22×10^{-3}	5.45×10^5	0.23
Pc-SA-5	1.00×10^{-2}	6.45×10^5	0.22

^a Determined by static laser light scattering. ^b Determined in CHCl₃ using unsubstituted zinc(II) phthalocyanine as the standard ($\Phi_f = 0.30$ in 1-chloronaphthalene).

were distilled from sodium and calcium chloride, respectively. Chloroform was distilled from calcium hydride. Acetic anhydride was distilled prior to use. Sebacic acid was recrystallized three times from ethanol. All other reagents and solvents were of reagent grade and used as received. Tetrahydroxyphthalocyaninatozinc(II) [ZnPc(OH)₄] (**1**) was synthesized by a literature procedure.¹⁶

Laser Light Scattering (LLS). A modified commercial LLS spectrometer (ALV/SP-125) equipped with a multi- τ digital time correlator (ALV-5000) and a solid-state diode laser (ADLAS DPY425II, output power ≈ 400 mW at $\lambda = 532$ nm) was used. In static LLS, the angular dependence of the excess absolute time-average scattered intensity, known as the Rayleigh ratio $R_{vv}(q)$, was measured. For a dilute dispersion at a relatively small scattering angle θ , $R_{vv}(q)$ can be related to the weight-average molar mass M_w , the second virial coefficient A_2 , and the z -average root-mean-square radius of gyration $\langle R_g^2 \rangle_z^{1/2}$ (or simply $\langle R_g \rangle$) by eq 1:

$$\frac{KC}{R_{vv}(q)} \approx \frac{1}{M_w} \left(1 + \frac{1}{3} \langle R_g^2 \rangle_z q^2 \right) + 2A_2 C \quad (1)$$

where $K = 4\pi^2 n^2 (\partial n / \partial C)^2 / (N_A \lambda_o^4)$ and $q = (4\pi n / \lambda_o) \sin(\theta/2)$ with n , $\partial n / \partial C$ ($\approx 0.201 \pm 0.005$ mL g⁻¹), N_A , and λ_o being the solvent refractive index, differential refractive index increment, Avogadro's number, and the wavelength of light in a vacuum, respectively. At $q \rightarrow 0$ and $C \rightarrow 0$, $R_{vv}(q) \approx KCM_w$. In dynamic LLS, the Laplace inversion of a measured intensity–intensity time correlation function $G^{(2)}(t, q)$ in the self-beating mode results in a line-width distribution $G(\Gamma)$. For a pure diffusive relaxation, $(\Gamma/q^2)_{q \rightarrow 0, C \rightarrow 0}$ is equal to the translational diffusion coefficient D , which is further related to the hydrodynamic radius R_h by the Stokes–Einstein equation $R_h = k_B T / (6\pi\eta D)$, with k_B , T , and η being the Boltzmann constant, the absolute temperature, and the solvent viscosity, respectively. All the measurements were carried out at 25.0 ± 0.1 °C. Details of the experimental setup and theory can be found elsewhere.¹⁷

Absorption and Fluorescence Spectroscopies. UV–vis and steady-state fluorescence spectra were taken on a Hitachi U-3300 spectrophotometer and a Hitachi F-4500 spectrofluorometer, respectively. The fluorescence quantum yields were determined from the equation $\Phi_{\text{sample}} = (F_{\text{sample}}/F_{\text{ref}})(A_{\text{ref}}/A_{\text{sample}}) - (n_{\text{sample}}^2/n_{\text{ref}}^2)\Phi_{\text{ref}}$, where F , A , and n are the measured fluorescence (area under the fluorescence spectra), the absorbance at 610 nm, and the refractive index of the solvent, respectively. The subscripts “sample” and “ref” denote the sample and the reference, respectively, and $\Phi_{\text{ref}} = 0.30$ for unsubstituted zinc(II) phthalocyanine in 1-chloronaphthalene.¹⁸ The data are collected in Table 1.

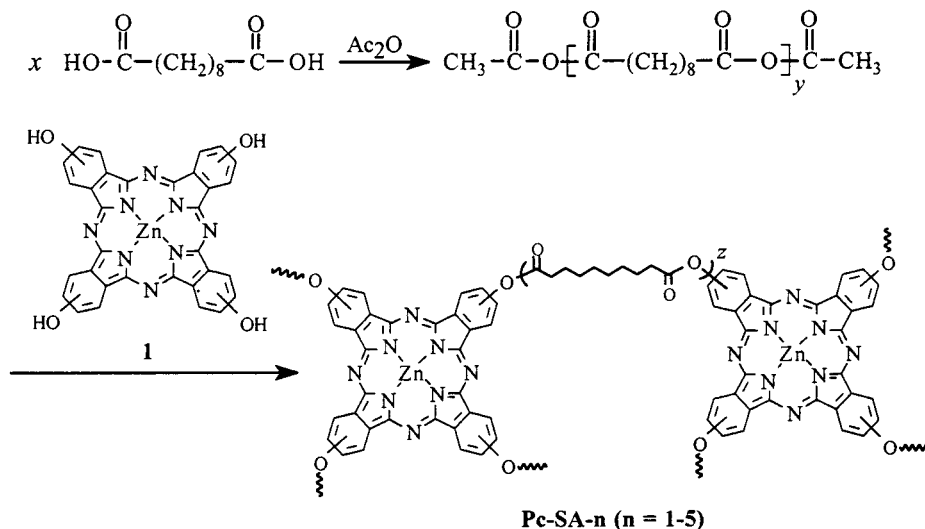
Sample Preparation. Sebacic acid was heated under reflux in acetic anhydride to give a mixture of oligo(anhydride), which

(16) (a) Leznoff, C. C.; Hu, M.; McArthur, C. R.; Qin, Y.; van Lier, J. E. *Can. J. Chem.* **1994**, *72*, 1990. (b) Hu, M.; Brasseur, N.; Yildiz, S. Z.; van Lier, J. E.; Leznoff, C. C. *J. Med. Chem.* **1998**, *41*, 1789.

(17) (a) Berne, B.; Pecora, R. *Dynamic Light Scattering*; Plenum Press: New York, 1976. (b) Chu, B. *Laser Light Scattering*, 2nd ed.; Academic Press: New York, 1991. (c) Wu, C.; Zhou, S. Q. *Macromolecules* **1995**, *28*, 8381. (d) Wu, C.; Zhou, S. Q. *Macromolecules* **1996**, *29*, 1574.

(18) Ferraudi, G. In *Phthalocyanines—Properties and Applications*; Leznoff, C. C., Lever, A. B. P., Eds.; VCH: New York, 1989; Vol. 1, p 301.

Scheme 1



was recrystallized from toluene and washed with *n*-hexane. The oligomers then underwent melted polycondensation with different amounts of ZnPc(OH)₄ (**1**) to give a series of poly(phthalocyanine-co-sebacic anhydrides) (Pc-SA-*n*) (*n* = 1–5) (Scheme 1). The crude products were dissolved in chloroform, and the undissolved materials were removed by filtration. The solutions were then rotary evaporated to give blue polymeric materials which were dried in vacuo. The IR spectra of all these copolymers as KBr pellets showed typical C=O stretchings for anhydrides at 1741 and 1809 cm⁻¹. Their weight-average molecular weights were also determined by static laser light scattering and are given in Table 1.

Nanoparticle Formation. A 1-mL dilute THF solution of Pc-SA-5 was added dropwise with constant stirring into 100 mL of water (purified by a Millipore system), containing the surfactant sodium dodecyl sulfate (SDS, ca. 1 cmc). Upon addition, THF diffuses and mixes with water quickly. The insoluble hydrophobic polymer chains collapse and aggregate in water to form nanoparticles. The small amount of THF in the mixture was then removed under reduced pressure to give SDS-stabilized Pc-SA-5 nanoparticles.

Degradation. In a typical degradation experiment, a proper amount of dust-free NaOH aqueous solution (clarified by a 0.1 μm Millipore filter) was added to a 2-mL dust-free suspension of Pc-SA-5 nanoparticles (clarified by a 0.8 μm Millipore filter). Both $R_{v,v}(q)$ and $G^{(2)}(t, q)$ were simultaneously measured during the degradation. Within the time scale, we did not see a significant effect of the NaOH solution on the stability of SDS. The release of Pc from the Pc-SA-5 nanoparticles was monitored by absorption and fluorescence spectroscopies.

Results and Discussion

The absorption spectra of the copolymers Pc-SA-*n* (*n* = 1–5) in chloroform given in Figure 1 are typical for monomeric phthalocyanines.^{6,9} The spectra show the B band at 343 nm, the Q band at 673 nm, and the two vibronic bands at 607 and 640 nm. As expected, the intensities of these bands are higher for copolymers with a higher Pc content. Upon excitation at 610 nm, all these copolymers fluoresce at ca. 680 nm. As shown in Table 1, the fluorescence quantum yield decreases initially with increasing Pc content, attaining a saturated value of ca. 0.22. This observation suggests that as the Pc content increases, the macrocycles in the polymer matrix exhibit a higher aggregation tendency.⁹

Figure 2 shows a typical Zimm plot for the SDS-stabilized Pc-SA-5 nanoparticles in water, which incorporates the angular and concentration dependence of the Rayleigh ratio $R_{v,v}(q)$ on a single grid. According to eq 1, the extrapolation of $[KC/R_{v,v}(q)]$ to $C \rightarrow 0$ and $q \rightarrow 0$ leads

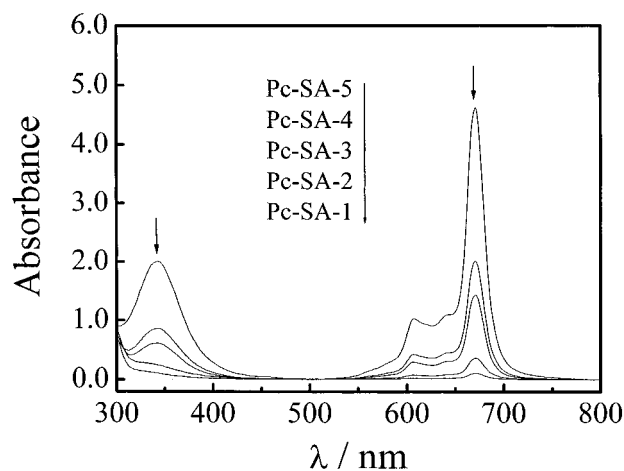


Figure 1. UV-vis spectra of Pc-SA-*n* (*n* = 1–5) in chloroform with a concentration of $3.30 \times 10^{-4} \text{ g cm}^{-3}$.

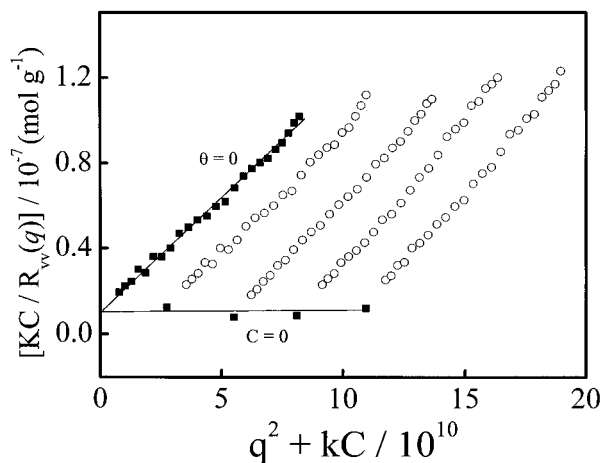


Figure 2. Typical Zimm plot for SDS-stabilized Pc-SA-5 nanoparticles in deionized water at 25 °C, where C ranges from 4.27×10^{-6} to $1.06 \times 10^{-5} \text{ g cm}^{-3}$.

to the value of M_w ($9.70 \times 10^7 \text{ g mol}^{-1}$), while the slopes for the lines plotting $[KC/R_{v,v}(q)]_{C \rightarrow 0}$ vs q^2 and $[KC/R_{v,v}(q)]_{q \rightarrow 0}$ vs C give the values of $\langle R_g \rangle$ (176 nm) and A_2 (≈ 0), respectively. From the values of M_w and $\langle R_h \rangle$, the average particle density $\langle \rho \rangle$ was estimated to be 0.084 g cm^{-3} , which is much smaller than that of a bulk polymer (ca. 1 g cm^{-3}). It shows clearly that the nanoparticles are

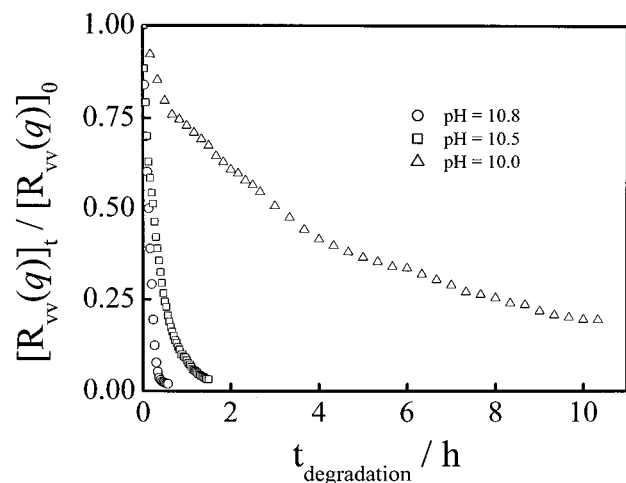


Figure 3. pH dependence of degradation of Pc-SA-5 nanoparticles at 25 °C, where initial nanoparticle concentration (C_0) = 5.41×10^{-5} g cm $^{-3}$.

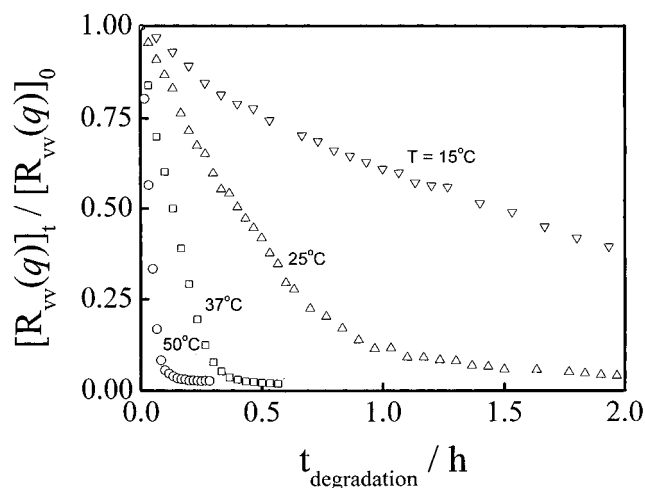


Figure 4. Temperature dependence of degradation of Pc-SA-5 nanoparticles at pH = 10.7, where initial nanoparticle concentration (C_0) = 5.41×10^{-5} g cm $^{-3}$.

composed of loosely aggregated polymer chains with a large number of water molecules entrapped inside.

The average hydrodynamic radius of the Pc-SA-5 nanoparticles in water was determined to be 166 nm by dynamic laser light scattering. It is known that the density distribution of a polymer chain in a colloid particle is reflected by the ratio of $\langle R_g \rangle / \langle R_h \rangle$.¹⁹ For a random coil chain in a good solvent, the ratio is around 1.5, while for a uniform sphere $\langle R_g \rangle / \langle R_h \rangle \approx 0.774$. The ratio for the SDS-stabilized Pc-SA-5 nanoparticles was ca. 1.06, indicating that the nanoparticles have a hyperbranching structure.²⁰ It agrees well with the low chain density $\langle \rho \rangle$.

The degradation of these nanoparticles was also studied by laser light scattering. Figures 3 and 4 show the decrease of $[R_{vv}(q)]_t / [R_{vv}(q)]_0$ during degradation at different pH values and temperatures, respectively. It is clear that the rate of degradation increases with the pH and temperature. The initial rate can be determined by a least-squares fitting of the initial linear region of each curve. At pH = 10.7, the initial rates at 15, 25, 37, and 50 °C were determined, giving a linear Arrhenius plot, from which

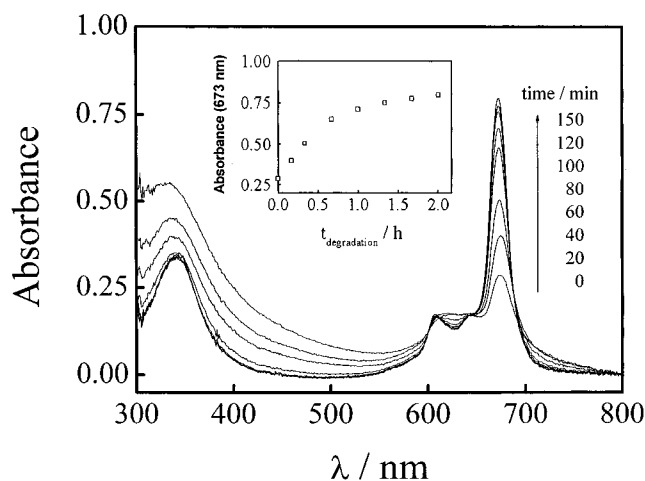


Figure 5. Changes in UV-vis spectrum during degradation of SDS-stabilized Pc-SA-5 nanoparticles at 25 °C, where C_0 = 5.41×10^{-5} g cm $^{-3}$ and pH = 10.7. The inset shows the degradation time dependence of the absorbance at 673 nm.

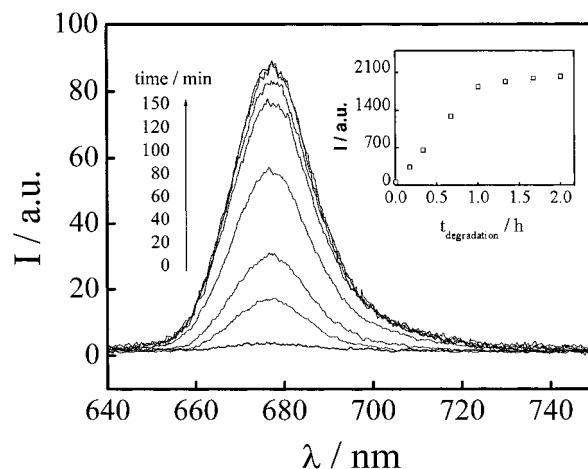


Figure 6. Changes in fluorescence spectrum during degradation of SDS-stabilized Pc-SA-5 nanoparticles at 25 °C, where C_0 = 5.41×10^{-5} g cm $^{-3}$ and pH = 10.7. The inset shows the degradation time dependence of the fluorescence intensity.

the activation energy for the degradation of these nanoparticles was found to be 72 kJ mol $^{-1}$. This value is much higher than that for the degradation of polymeric nanoparticles prepared from poly(ethylene oxide-*b*-sebacic anhydride) (44 kJ mol $^{-1}$).^{15c}

Figures 5 and 6 show the changes in absorption and fluorescence spectra of Pc-SA-5 nanoparticles during the degradation process. Initially (at $t = 0$), the Pc rings are highly aggregated as shown by the weak Q band absorption and fluorescence emission. This may be due to the collapse of polymer chains during the formation of nanoparticles in water. Upon degradation, the nanoparticles degrade into smaller degradation products that along with the surfactant SDS inhibit the aggregation of phthalocyanine, leading to a stronger Q band and a more intense fluorescence. The insets in Figures 5 and 6 show respectively the time dependence of the absorbance at the Q band (673 nm) and the fluorescence intensity during the degradation. It is clear that the release of phthalocyanine occurs almost immediately after the degradation of the nanoparticles.

In summary, we have prepared a novel series of phthalocyanine-containing biodegradable copolymers based on sebacic anhydride, and micronized one of these

(19) Tu, Y.; Wan, X.; Zhang, D.; Zhou, Q.; Wu, C. *J. Am. Chem. Soc.* **2000**, *122*, 10201.

(20) Wu, C.; Zuo, J.; Chu, B. *Macromolecules* **1989**, *22*, 633.

copolymers (Pc-SA-5) into nanoparticles via a microphase inversion method. The degradation of these nanoparticles and the release of phthalocyanine have been monitored by a combination of laser light scattering and absorption and fluorescence spectroscopies. The results show that this biocompatible polymer-based colloidal system is potentially useful for the delivery and release of photosensitizers in PDT.

Acknowledgment. This work was supported by the Research Grants Council of the Hong Kong Special Administrative Region, China (RGC Ref. No. CUHK 4181/97P, CUHK 4117/98P, and CUHK 4309/99P). J.F. and X.L. thank The Chinese University of Hong Kong for partial support of a postdoctoral fellowship.

LA011764A